This is a preprint, the final version is subject to change, of the American Mineralogist (MSA)
Cite as Authors (Year) Title. American Mineralogist, in press.
(DOI will not work until issue is live.) DOI: http://dx.doi.org/10.2138/am-2016-5567

Revision 1

A Cr^{3+} luminescence study of spodumene at high pressures: Effects of site geometry, a phase transition and a level-crossing

Earl O'Bannon III and Quentin Williams

Department of Earth and Planetary Sciences, University of California, Santa Cruz, 1156 High Street, Santa Cruz, California 95064, U.S.A.

Abstract

Cr^{3+} luminescence of the green Cr-bearing variety of spodumene ($LiAlSi_2O_6$) has been studied under hydrostatic conditions up to ~15 GPa. R-line luminescence is a particularly sensitive site-specific probe of the Al-site, and high-pressure phase transitions that affect the symmetry or electron density at this site should produce obvious changes in the luminescence spectra. Thus, the nature of Cr^{3+} luminescence is probed across known and possible phase transitions in spodumene. Discontinuous shifts of the R-lines and their sidebands to higher energy at 3.2 GPa are associated with the C2/c to $P2_1/c$ phase transition. Both R-lines and sidebands shift to lower energy after the 3.2 GPa transition up to ~15 GPa. The C2/c to $P2_1/c$ phase transition is confirmed to be first order in nature based on its observed hysteresis on decompression, and R-line and sideband measurements give no evidence of a second proposed transition up to ~15 GPa. The splitting between the R_1 and R_2 bands is dramatically enhanced by pressure, with the split decreasing at the phase transition. These trends correspond to pressure-induced shifts in the distortion of the M1 site, and a likely shift in off-centeredness of the Cr^{3+} ion. Pressure-induced decreases in linewidths are consistent with the R-lines shifting at slower rates than the phonons to which they are most closely coupled, as demonstrated by large

Always consult and cite the final, published document. See http:/www.minsocam.org or GeoscienceWorld

pressure shifts of vibronic peaks. Observations of a pressure-induced cross-over between the $^4T_2$ and ^2E levels of the Cr^{3+} ion indicate that spodumene undergoes a shift from an intermediate strength crystal field environment to a high strength crystal field environment at pressures between ambient and 3.2 GPa.

Keyword: spodumene, pyroxene, high-pressure, phase transition, Cr^{3+} luminescence

Introduction

Spodumene ($LiAlSi_2O_6$) is a lithium bearing pyroxene that crystallizes in the monoclinic crystal system with C2/c symmetry. Pyroxenes are major rock-forming minerals in the Earth's crust, and the upper mantle. While spodumene is certainly not abundant in the Earth's crust and upper mantle, understanding high-pressure phase transitions in C2/c pyroxenes is important for understanding the high-pressure behavior of mantle relevant pyroxenes (e.g. hedenbergite and diopside), and hence the structure of the upper mantle. High-pressure phase transitions in spodumene have been extensively studied (Arlt & Angel 2000; Pommier et al. 2003; Nestola et al. 2008; Ullrich et al. 2009). The first-order displacive C2/c to $P2_1/c$ phase transition in spodumene occurs at ~3.2 GPa and is generally well agreed upon (Figure 1). One study (Pommier et al. 2003) reports a possible higher pressure isosymmetric phase transition in the 7.7-10.5 GPa range based on shifts in the Raman spectra of this phase, and propose this phase transition is associated with a change in the lithium coordination number from five to six.

Arlt and Angel (2000) used single crystal x-ray diffraction and did not report a second phase transition in spodumene up to 8.8 GPa. They do suggest that a second phase transition is likely above 10 GPa based on the high-pressure kink value of the B chain (Figure 1). Similarly, Ullrich et al. (2009) performed both single crystal X-ray diffraction

Always consult and cite the final, published document. See http:/www.minsocam.org or GeoscienceWorld

and Raman spectroscopy of spodumene up to ~9.24 GPa and concluded that a second transition at 7.7 GPa is unlikely. Among closely related materials, a Raman and x-ray investigation of $LiFeSi_2O_6$ by Pommier et al. (2005) reported a C2/c to $P2_1/c$ phase transition between 0.7 and 1.0 GPa. They also suggest possible spin crossovers at ~6.0 GPa and propose that the disappearance of several peaks in the Raman spectrum (similar to the disappearance of peaks in the spodumene Raman spectra at high pressure) at ~8.0 GPa is evidence of a $P2_1/c$ to $P2_1/c$ phase transition. Nestola et al. (2008) used x-ray diffraction to examine $Li(Al_{0.53}Ga_{0.47})Si_2O_6$ and $LiGaSi_2O_6$ and found that the C2/c to $P2_1/c$ phase transition occurs between ~1.8 and 2.1 GPa in the mixed sample and between 0.0001 and 0.4 GPa in the Ga end-member. The mixed sample was studied up to ~9.0 GPa and the Ga end-member up to ~7.5 GPa and no higher pressure phase transitions were reported.

We utilize the fluorescence of chromium to probe the response of spodumene to pressure: such fluorescence under pressure is well-characterized for ruby, whose role as a pressure calibrant is well-known (e.g., Mao and Bell, 1986), but few other minerals have had the fluorescence of Cr^{3+} dopants examined under pressure (alexandrite, MgO, and $MgAl_2O_4$ are notable exceptions: Kottke and Williams, 1983; Jahren et al., 1990; Chopelas, 1996; Jovanic, 2000). Notably, most other oxide minerals examined to date under pressure utilizing Cr^{3+} fluorescence have nearly ideal octahedral or only slightly distorted Cr-bearing sites. Spodumene's M1 site is, in comparison, substantially distorted (e.g., Clark et al., 1968; Arlt and Angel, 2000). Hence, spodumene allows both the interrogation of the fluorescent response of Cr under pressure within a notably distorted site, and also through a phase transition at moderate pressures.

Always consult and cite the final, published document. See http:/www.minsocam.org or GeoscienceWorld

Characteristically, such fluorescence spectra show the strong and relatively sharp R-lines associated with the spin-forbidden ^2E-$^4A_2$ transition, with the $^4A_2$ state being the ground state and the ^2E state being split in non-cubic environments (Syassen, 2008). At low crystal-field strengths, (e.g., Tanabe and Sugano, 1954), the generally broader $^4T_2$-$^4A_2$ emission may dominate the emission spectrum; at intermediate field strengths, it may be present in the spectrum with the R-lines; and at high field strengths, the narrow band ^2E-$^4A_2$ emission dominates the fluorescence spectrum. In addition, vibronic bands are also observed: these phonon-associated sidebands are offset from the R-lines by the frequency of a coupled vibrational mode. Finally, comparatively sharp (and low amplitude in samples with dilute Cr^{3+} substitution) neighbor lines, generated by shared excitations between neighboring Cr^{3+} centers, are also observed: these bands tend to be complex, since a wide variety of potential neighbor interactions exist. If their assignments are known, their pressure-dependence can be used to estimate changes in magnetic interactions between chromium centers (e.g., Williams and Jeanloz, 1985).

Here, we use Cr^{3+} luminescence as a probe of the Al-site in spodumene under high-pressure. The luminescence spectra of the high pressure phase(s) of spodumene have not been previously reported. Thus, our experiments are oriented towards: (1) determining if luminescence spectra can elucidate high-pressure phase transitions in spodumene (in particular the proposed transition in the 7.7-10.5 GPa range); (2) characterize the luminescence spectra of the high pressure phases of spodumene; and (3) measure the pressure shift of the R-lines and sidebands.

Experimental Methods

Always consult and cite the final, published document. See http:/www.minsocam.org or GeoscienceWorld

Our sample was a natural light green gem quality spodumene from Minas Gerais, Brazil obtained from the UCSC mineral collection (#6744: colloquially, such a spodumene is often referred to as hiddenite). The sample is a single crystal with dimensions of ~3.0 x 2.0 x 0.5 cm and displays typical 90° pyroxene cleavage. Sample purity was confirmed by Raman spectroscopy and luminescence spectroscopy, which were in excellent agreement with previous studies (Pommier et al. 2003; Walker et al. 1997). Chromium content was measured with a PhotonMachines Analyte 193H, which is a 193 nm ArF excimer laser system coupled with a ThermoScientific ElementXR single-collector magnetic sector ICP-MS. The instrument was calibrated with a SRM 610 trace element glass from NIST. The average chromium content was found to be 31.0 (±5.1) ppm.

High static pressures were generated using a Merrill-Bassett type diamond anvil cell (DAC) equipped with 16-sided type Ia 500 μm culet diamond anvils. A spring steel gasket with a 200 μm hole was used as the sample compartment. Experiments were carried out with methanol:ethanol:water 16:3:1 and methanol:ethanol 4:1 mixtures as the pressure media, which yield hydrostatic conditions up to the maximum pressure of this study (Piermarini et al. 1973; Fujishiro et al. 1982; Angel et al. 2007; Klotz et al. 2009). One single crystal of spodumene and one single crystal of ruby were loaded into the sample compartment for each experiment. Four experiments were conducted (three in 16:3:1 M:E:W and one in 4:1 M:E) and each experiment consisted of one compression and decompression cycle. Results of the different pressure media are indistinguishable from one another. The standard ruby fluorescence method (Mao & Bell 1986) was used to determine the pressure.

Always consult and cite the final, published document. See http:/www.minsocam.org or GeoscienceWorld

For the low temperature measurements, the sample was immersed in liquid nitrogen. For the high-temperature measurements, the sample was heated using a modified DAC external heater previously described in Kraft et al. (1991). Temperatures in the high-temperature experiments were measured using a thermocouple attached directly to the sample with silver paint. This technique yields uncertainties of ±3.0 K.

Luminescence spectra were collected from 650-800 nm (15380-12500 cm^{-1}) with a Horiba LabRAM HR Evolution Raman spectrometer with a spectrometer focal length of 800 mm. Spectra were collected to a pressure of ~15 GPa and on decompression at 298 K using an excitation wavelength of 532 nm. An Olympus BXFM-ILHS microscope with a 50x long working distance objective was used to focus the laser beam onto the sample. An 1800 lines/mm grating with a corresponding spectral resolution of ~1 cm^{-1} (or, equivalently, ~0.05 nm) was utilized. Combinations of Gaussian and Lorentzian functions were fit to the luminescence spectra with Horiba Labspec6 software.

Results and discussion

Representative luminescence spectra of spodumene on compression to ~15 GPa and on decompression to room pressure are shown in Figure 2. The pressure shifts of the R-lines and sidebands are plotted in Figure 3a & b (band positions as a function of pressure are included in supplementary material). In the C2/c phase, two peaks are fit under each of the primary R_1 and R_2 bands. The more intense of each of the two fit components of the R_1 and R_2 bands lies on the lower wavelength side of the strong R-related peaks observed. The higher wavelength fit components of these peaks are smaller in amplitude and appear as shoulders/asymmetry on the high wavelength side of these bands (Fig. 3a).

Always consult and cite the final, published document. See http:/www.minsocam.org or GeoscienceWorld

In the $P2_1/c$ phase, three peaks are fit under the R_1 band, and two peaks are fit under R_2. These additional, low amplitude shoulders may be associated with either R-line emissions associated with chrome centers subject to modest lattice distortion accompanying the substitution of a nearby Cr^{3+} ion in the M1-octahedral chains, or be produced by a neighbor line that lies close to the R-line emissions. The latter interpretation plausibly explains the higher wavelength peak associated with the R_1 band in the high-pressure phase: this band becomes visible as the R-lines narrow through the phase transition. Figure 3 and Table 1 report the pressure shifts of the R-lines and sidebands in each polymorph of spodumene. Both components of the R_1 band shift positively in wavelength up to the 3.2 GPa transition, while both R_2 components shift slightly negatively in wavelength. Both R-lines shift positively in wavelength following the 3.2 GPa transition up to the maximum pressure of the study.

At 298K, sharp R-line emissions with an R_2 line at 686.54 nm (14565.8 cm^{-1}) and R_1 at 690.55 nm (14481.2 cm^{-1}), a broad $^4T_2$-$^4A_2$ transition at ~730.02 nm (13698.5 cm^{-1}), and phonon sidebands are observed (Figure 4). At 77 K, the R-lines shift to 685.14 nm (14595.6 cm^{-1}) for R_2, and 689.40 nm (14505.4 cm^{-1}) for R_1, and the intensity of the $^4T_2$-$^4A_2$ transition drops to unresolvable amplitude, implying that this transition is induced by thermal population of the $^4T_2$ state: this assignment and observation agrees well the ambient pressure spectra and interpretation of Walker et al. (1997). At 373 K, the R_2 band shifts to 686.83 nm (14559.6 cm^{-1}) and R_1 shifts to 691.41 nm (14463.2 cm^{-1}). Even with this modest temperature increase, notable broadening of the R-lines is observed (R_2 becomes a shoulder), and the intensity of the $^4T_2$ transition increases (relative to the R_1 band). This progressive thermally-activated marked growth of the $^4T_2$-$^4A_2$ transition and its

Always consult and cite the final, published document. See http:/www.minsocam.org or GeoscienceWorld

158 coexistence with the R-lines indicate that the ^2E and $^4T_2$ states are reaching thermal
159 equilibrium—a phenomenon observed in other oxides, such as ruby, emerald and topaz
160 (e.g., Kisliuk and Moore 1967; Taraschan et al. 2006). Moreover, that the energies of the ^2E
161 and $^4T_2$ states lie close to one another indicates that the Cr site in spodumene is in an
162 intermediate strength crystal field environment.
163 Indeed, a similar, but more extreme, temperature dependence of Cr^{3+}-emission
164 spectra has been observed in gadolinium scandium gallium garnet (GSGG). Henderson et al.
165 (1988) report that below 70K, the ^2E is the lowest excited state of the Cr^{3+} ion, while at
166 300K the $^4T_2$ level lies lower than the ^2E state by about 150 cm^{-1}. In this case, they propose
167 that it is the thermal expansion that reduces the energy level splitting between ^2E and $^4T_2$
168 excited states. Comparable effects are observed in this system under compression, as well,
169 as the $^4T_2$ emission is dramatically decreased under compression (Hommerich and Bray
170 1995). The two key aspects of these strong temperature and pressure dependences of
171 emission intensities that are relevant to spodumene are that: (1) the ^2E and $^4T_2$ states are
172 strongly spin-orbit coupled, and admixed with one another, due to their close proximity;
173 and (2) the relative amplitudes of emission from the ^2E and $^4T_2$ states varies as $\Delta[E(^4T_2)$-
174 $E(^2E)]$ (Kisliuk and Moore 1967; Hommerich and Bray 1995). In this difference term, $E(^4T_2$,
175 $^2E)$ represent the respective energies of the two electronic states: when Δ is substantially
176 greater than 0, sharp R-line fluorescence predominates and the system is strong field; weak
177 field conditions occur when Δ is less than zero, producing broad-band $4T_2$-related
178 emission.
179 Although the high temperature behavior of pyroxenes can be complex (e.g., kanoite
180 ($MnMgSi_2O_6$) undergoes a $P2_1/c$ to $C2/c$ transition at ~240 ^oC: Arlt and Armbruster 1997),

Always consult and cite the final, published document. See http:/www.minsocam.org or GeoscienceWorld

spodumene is known to remain in the C2/c structure when heated to at least 760 °C (Cameron et al. 1973). Hence, high temperature phase transitions do not play a role in the high temperature luminescence behavior. Notably, the $^4T_2$ band's location at ~730.02 nm at room pressure and temperature is at substantially longer wavelength than the corresponding absorption of this transition near 628 nm (Khomenko and Platonov 1985). Thus, the excited state of this transition is Stokes shifted to the long wavelength side of the R-lines, a phenomenon that is well-documented in, for example, both emerald and ruby (Kisliuk and Moore, 1967).

The $^4T_2$-$^4A_2$ emission intensity decreases in amplitude dramatically under compression, and shifts to higher frequency/lower wavelength rapidly (at ~100 cm^{-1}/GPa: Figure 5). Its broad emission is resolvable up to the ~3.2 GPa transition on compression, but becomes difficult to resolve in the $P2_1/c$ phase. This transition corresponds to the difference in energy between the split *d* orbitals of the chromium ion, and is represented as 10Dq. If we assume, in accord with an octahedral crystal-field point-charge model, that this scales as $R^{-5}_{Cr\text{-}O}$ (e.g., Zheng, 1995; Bray, 2001), then we derive a contraction in the $R_{Cr\text{-}O}$ distance of ~0.5% at 3 GPa. This result is in gross accord with the ~0.7% decrease observed for the Al-O distances by Arlt and Angel (2000) between 0 and 3 GPa. However, the roles of site distortion/deviation from an octahedral environment, pressure-induced shifts in site-geometry (including changes in off-centeredness of ions within the site), and spin-orbit coupling and admixture between the $^4T_2$ and ^2E levels render such octahedral point charge-based scaling results suspect for spodumene.

The decrease in intensity of the $^4T_2$-$^4A_2$ emission is clearly due to a transition in the crystal field strength from intermediate to strong, as manifested by the energetic cross-

Always consult and cite the final, published document. See http:/www.minsocam.org or GeoscienceWorld

over of the $^4T_2$ and ^2E states in the d^3 Tanabe-Sugano diagram (Gaft et al. 2005 and Figure 6). Such a transition from predominantly broad-band to narrow-band fluorescence has been previously characterized in a number of Cr^{3+}-bearing materials under pressure, and particularly fluorides and gallium-based garnets (e.g., Dolan et al., 1986; de Viry et al., 1987; Freire et al., 1994; Hommerich and Bray, 1995; Grinberg and Suchocki, 2007; Sanz-Ortiz et al., 2010). This transition, in which spodumene starts in an intermediate crystal-field strength state (as indicated by both the close proximity of the $^4T_2$-$^4A_2$ and ^2E-$^4A_2$ emission peaks and the coexistence of their respective broad-band and narrow-band emissions), proceeds towards a strong-field strength state relatively rapidly under pressure. By 3 GPa, the markedly lower amplitude $^4T_2$ state has nearly crossed-over in energy with the ^2E state (Figures 5 and 6). We are unaware of any other reports of such a pressure-induced level cross-over in an oxide mineral, and these results illustrate the ability to, under appropriate circumstances, precisely locate the strength and pressure-dependence of crystal-field strength utilizing fluorescence spectra under pressure.

In the sideband region (Figure 3b), twelve bands can be resolved up to the ~3.2 GPa transition, and above the transition nine bands can be resolved up to the maximum pressure of this study. Within the C2/c phase, all the sidebands shift initially negatively in energy, with a decrease in the absolute values of their shifts starting at ~1.2 GPa, followed by a change in sign at ~2.2 GPa (Fig. 3b). These indications of non-linearities in some of the sideband mode shifts in the region below 3 GPa are likely associated with the migration of the $^4T_2$ state through this spectral region: complex Fano-type resonances have been observed to occur associated with the pressure-induced interaction of the $^4T_2$ state with lower-lying electronic states (Sanz-Ortiz et al., 2010). At the phase transition at ~3.2 GPa,

Always consult and cite the final, published document. See http:/www.minsocam.org or GeoscienceWorld

all of the sidebands shift discontinuously to shorter wavelength (higher energy). After the ~3.2 GPa transition, the sidebands shift positively in wavelength (to lower energy) and linearly up to ~15 GPa. On decompression, all sidebands show hysteresis across the ~3.2 GPa transition, providing additional confirmation that this transition is first-order in character (Arlt and Angel, 2000; Ullrich et al., 2009).

3.2 GPa transition

Both components of the R-lines in the C2/c phase undergo discontinuous shifts (Figure 3a) to higher energy at ~3.2 GPa. The R_1 band shifts by -1.88 nm (+39 cm^{-1}) and R_2 shifts by -1.26 nm (+27 cm^{-1}). Arlt and Angel (2000) investigated this phase transition with single crystal X-ray diffraction and reported that the *a*- and *c*- unit cell parameters decrease in length while the *b*- unit cell parameter increases in length across this transition. The net result is a decrease in volume of the unit cell with an increase in the volume of the Al-octahedron. The shifts of the R-lines to higher energy, coupled with their negative pressure shifts, are consistent with this increase in volume of the Al-octahedron. Sidebands also undergo a similar discontinuous shift to higher energy (Figure 3b) across the transition. On decompression in the 3.2-2.0 GPa range, R-lines from both the $P2_1/c$ and C2/c spodumene phases are present in the spectra. This indicates that on decompression across the ~3.2 GPa transition, the low-pressure and high-pressure phases of spodumene coexist in closely juxtaposed sub-domains.

R-Line Separation and their FWHM

The R-line separation increases markedly as a function of pressure in the C2/c and $P2_1/c$ phase (Figure 7a). Room pressure single crystal x-ray diffraction data indicates that the Al-sites in spodumene are quite distorted (Clark et al. 1968, Cameron et al. 1973,

Always consult and cite the final, published document. See http:/www.minsocam.org or GeoscienceWorld

Tribaudino et al. 2003, Redhammer and Roth 2004). High pressure single crystal x-ray data indicates that the Al-octahedron may become slightly more distorted up to the 3.2 GPa transition (Arlt and Angel, 2000: Figure 7a, inset) and, after the transition, the Al-octahedra become substantially more distorted with pressure, as measured by the quadratic elongation of the octahedron (Robinson et al. 1971). Quadratic elongation is a measure of polyhedral distortion that is independent of the effective size of the polyhedra, and which closely correlates with polyhedral angle variance (Robinson et al. 1971). The splitting of the R-lines is generally viewed in (for example) ruby as being a consequence of the trigonal distortion in the aluminum site in Al_2O_3 (Syassen, 2008). Thus, the dramatic increase in R-line separation with pressure in the low-pressure phase appears, given the modest (at best) increase in site distortion in this phase, to be anomalous. Refinements of the M1-site show, however, that the Al^{3+} ion in spodumene is substantially off-center within this site (Figure 1), and that the effect of pressure is to enhance this off-centered character via migration of the Al-ion along the *b*-axis of the structure (Arlt and Angel, 2000). We anticipate that comparable off-centeredness, and a pressure-induced shift in off-centeredness, may accompany chromium substitution in this site. We therefore propose that the notable change in R-line splitting in the low-pressure phase is due to a pressure-induced shift in the off-centeredness of the chromium ion in this site.

Indeed, Taran et al. (2011) note, based on optical absorption spectra, that a substantial amount of local lattice relaxation appears to accompany Cr substitution into the M1 site of (particularly) Li-pyroxenes. Specifically, the relaxation parameter of chromium in spodumene, ε (Ardit et al., 2014), is defined as $((Cr\text{-}O)^{local}\text{-}(Al\text{-}O)/((Cr\text{-}O)^{endmember}\text{-}(Al\text{-}O))$, where $(Cr\text{-}O)^{local}$ is the bond length of dilute chromium substituents in spodumene as

Always consult and cite the final, published document. See http:/www.minsocam.org or GeoscienceWorld

273 estimated from optical absorption spectra, and $(Cr\text{-}O)^{endmember}$ is that of $LiCrSi_2O_6$. Using
274 data quoted in Taran et al. (2011) and the zero pressure Al-O distance for spodumene from
275 Arlt and Angel (2000), the value of ε for spodumene is indistinguishable from 1, implying
276 that chromium substitution induces extensive local distortion: it substitutes in at an ionic
277 radius of near 1.99 Å into a site for which the average M1 (Al-O) distance is 1.92 Å. Hence,
278 local distortion is particularly large for Cr-substitution into spodumene, and the Cr^{3+} site
279 itself may have anomalous distortions that are not captured by single-crystal diffraction
280 experiments on spodumene. X-ray absorption experiments are likely required to fully
281 characterize the nature and magnitude of these local distortions and off-centered
282 character, but our luminescence data are most readily explained by a significant pressure
283 dependence of the off-centeredness of chromium.
284 The FWHM (full width at half-maximum) as a function of pressure is shown in
285 Figure 7b. The FWHM of the R-lines in C2/c phase decreases as pressure increases, and at
286 the 3.2 GPa transition, the FWHM of both R-lines decreases. In the $P2_1/c$ phase, the FWHM
287 of the R-lines initially decreases as pressure is increased up to ~6.0 GPa, and then increases
288 slightly up to the maximum pressure of this study. On decompression, the FWHM of the R-
289 lines follows generally the same trend as they did during compression, although the scatter
290 is substantially greater, possibly due to the effects of residual strain following
291 decompression. As Kottke and Williams (1983) describe, the pressure-dependence of the
292 linewidth of R-lines can be modeled using a Debye-based model, modified from the
293 temperature-dependence of linewidths proposed by Imbusch et al. (1964). The pressure
294 shifts of the vibronic peaks are rapid, with migration rates away from the R-lines (Table 1)
295 that are substantially in excess of the rate at which Raman-active modes in spodumene

Always consult and cite the final, published document. See http:/www.minsocam.org or GeoscienceWorld

shift with pressure (Pommier et al., 2003). Although the vibrations coupling with the electronic transition are expected to be of odd parity (Sangster and McCombie, 1970), infrared-active vibrations are anticipated to have roughly comparable pressure shifts to the Raman vibrations. This increased separation with pressure implies that the coupling of phonons with the R-lines decreases with pressure over the pressure range of these measurements, which is consistent with our observations of narrowing linewidths under pressure. The underpinning reason for the rapid shifts of the vibronic lines is not entirely apparent. We speculate that the large volume of the Cr^{3+} ion within the M1 octahedral site and associated local distortions (and shifts in off-centeredness) may generate more rapid pressure shifts of vibrations associated with the Cr^{3+} site. This possibility implicitly suggests that the vibronic peaks in spodumene are associated with local vibrational modes rather than vibrational modes of the bulk lattice. This suggestion is in accord with simulations of coupling of vibrations with electronic transitions of isovalent substitutions in MgO (e.g., Sangster and McCombie, 1970).

Implications

The sensitivity of R-line luminescence to changes in the local bonding environment of the Al-site is clearly demonstrated by the discontinuous shift of the R-lines and sideband features at ~3.2 GPa. No discontinuous changes in the luminescence spectra from 3.2 GPa to ~15 GPa were observed, showing that a second phase transition in the ~7.7-10.5 GPa region is unlikely. We note that if the proposed ~7.7-10.5 GPa transition primarily involves subtle changes in the local bonding environment of the M2 site (Li-site), and the M1 sites (Al-sites) remain more or less unchanged, this might not substantively change the character of the R-line luminescence. However, given the high sensitivity of R-line emission

Always consult and cite the final, published document. See http:/www.minsocam.org or GeoscienceWorld

to subtle changes in Al-site volume, distortion, and/or electron density, a structural change that occurs absent a shift in R-line fluorescence seems unlikely (Wamsley and Bray 1994; Syassen 2008). In summary, the clear discontinuity associated with the phase transition of spodumene within the R-line fluorescence, and the systematic and monotonic behavior of the R-lines and their sidebands at pressures above the transition, demonstrate both the sensitivity of R-lines to structural changes within the crystal, and the (possible meta-) stability of the $P2_1/c$ phase at 298 K to higher pressures than has previously been documented.

These measurements constrain the strength and pressure dependence of the crystal field strength in spodumene. We also demonstrate that pressure induced shifts in the off-centeredness of the chromium ion likely contribute to the increase in R-line splitting in the C2/c phase (shifts in site distortion are not the sole consideration in generating R-line splitting). These observations illustrate the utility of Cr^{3+}-luminescence as a site specific probe in minerals, and specifically the value of high pressure luminescence measurements: even within a highly distorted octahedral site, such as the Al-site in spodumene, constraints on local bonding and crystal field strength can be generated. Finally, such luminescence measurements can expand the known stability (or metastability) range of complex crystalline phases of relevance to the upper mantle, such as the extension of the persistence of the $P2_1/c$ phase of spodumene at 298 K to ~15 GPa.

Acknowledgements

Helpful discussions with C. Vennari and C. Stan as well as comments from M. Taran, an anonymous reviewer, and the Associate Editor (S. Speziale) greatly improved the quality of the manuscript. We thank Dan Sampson for invaluable technical assistance with the

Always consult and cite the final, published document. See http:/www.minsocam.org or GeoscienceWorld

Raman spectrometer and heating apparatus. Work partially supported by NSF through EAR-1215745, and COMPRES, the Consortium for Materials Properties Research in Earth Sciences under NSF Cooperative Agreement EAR 11-57758.

References

Angel, R.J. Bujak, M., Zhao, J., Gatta, G.D., and Jacobsen, S.D. (2007) Effective hydrostatic limits of pressure media for high-pressure crystallographic studies. Journal of Applied Crystallography, 40, 26–32.

Ardit, M., Dondi, M., and Cruciani, G. (2014) On the structural relaxation around Cr^{3+} along binary solid solutions, European Journal of Mineralogy, 26, 359-370.

Arlt, T., and Angel, R.J. (2000) Displacive phase transitions in C-centred clinopyroxenes: spodumene, $LiScSi_2O_6$ and $ZnSiO_3$. Physics and Chemistry of Minerals, 27, 719–731.

Arlt, T., and Armbruster, T. (1997) The temperature-dependent $P2_1/c$-$C2/c$ phase transition in the clinopyroxene kanoite $MnMg[Si_2O_6]$: a single-crystal X-ray and optical study. European Journal of Mineralogy, 953-964.

Bray, K.L. (2001) High pressure probes of electronic structure and luminescence properties of transition metal and lanthanide systems, Topics in Current Chemistry, 213, 1-94.

Cameron, M., Sueno, S., Prewitt, C.T., and Papike, J.J. (1973) High-temperature crystal chemistry of acmite, diopside, hedenbergite, jadeite, spodumene, and ureyite. American Mineralogist, 58, 594-618.

Chopelas, A. (1996) The fluorescence sideband method for obtaining acoustic velocities at high compressions: Application to MgO and $MgAl_2O_4$. Physics and Chemistry of Minerals, 23, 25-37.

Clark, J.R., Appleman, D.E., and Papike, J.J. (1968) Bonding in eight ordered clinopyroxenes isostructural with diopside. Contributions to Mineralogy and Petrology, 20, 81-85.

de Viry, D., Denis, J.P., Tercier, N., and Blanzat, B. (1987) Effect of pressure on trivalent chromium photoluminescence in fluoride garnet $Na_3In_2Li_3F_{12}$, Solid State Communications, 63, 1183-1188.

Dolan, J.F., Kappers, L.A., and Bartram, R.H. (1987) Pressure and temperature dependence of chromium photoluminescence in K_2NaGaF_6:Cr^{3+}, Physical Review B, 33, 7339-7341.

Freire, P.T.C., Pilla, O., and Lemos, V. (1994) Pressure-induced level crossing in $KZnF_3$:Cr^{3+}, Physical Review B, 49, 9232-9235.

Always consult and cite the final, published document. See http:/www.minsocam.org or GeoscienceWorld

373 Fujii, A.T., and Isotani, S. (1988) Optical absorption study of five varieties of spodumene,
374 Anais da Academia Brasileira de Ciencias, 60, 127-135.

375 Fujishiro, I., Piermarini, G.J., Block, S., and Munro, R.G. (1982) Viscosities and glass
376 transition pressures in the methanol-ethanol-water system. High Pressure Research in
377 Science and Industry: Proceedings of the 8th AIRAPT Conference, 2, pp. 608–611.

378 Gaft, M., Reisfeld, R., and Panczer, G. (2005) Modern Luminescence Spectroscopy of
379 Minerals and Materials, 356 pp. Springer-Verlag, Berlin.

380 Grinberg, M., and Suchocki A. (2007) Pressure-induced changes in the energetic structure
381 of the $3d^3$ ions in solid matrices. Journal of Luminescence, 125, 97-103.

382 Henderson, B., Marshall, A., Yamaga, M., O'Donnell, K.P., and Cockayne, B. (1988) The
383 temperature dependence of Cr^{3+} photoluminescence in some garnet crystals. Journal
384 of Physics C 21, 6187-6198.

385 Hommerich, U., and Bray, K.L. (1994) High-pressure laser spectroscopy of
386 Cr^{3+}:$Gd_3Sc_2Ga_3O_{12}$ and Cr^{3+}:$Gd_3Ga_5O_{12}$, Physical Review B, 51, 12133-12141.

387 Imbusch, G.F., Yen, W.M., Schawlow, A.L., McCumber, D.E., and Sturge, M.D. (1964)
388 Temperature dependence of the width and position of the ^2E -> $^4A_2$ fluorescence lines
389 of Cr^{3+} and V^{2+} in MgO, Physical Review, 133, 1029-1034.

390 Jahren, A.H., Kruger, M.B., and Jeanloz, R. (1992) Alexandrite as a high-temperature
391 pressure calibrant, and implications for the ruby-fluorescence scale, Journal of Applied
392 Physics, 71, 1579-1584.

393 Jovanić, B.R. (2000) Effect of high pressure on fluorescence lifetime and position for R1 line
394 in synthetic spinel $MgAl_2O_4$:Cr^{3+}, Materials Science Forum, 352, 247-250, 2000.

395 Khomenko, V.M., and Platonov, A.N. (1985) Electronic absorption spectra of Cr^{3+} ions in
396 natural clinopyroxenes, Physics and Chemistry of Minerals, 11, 261-265.

397 Kisliuk, P., and Moore, C.A. (1967) Radiation from the $^2T_4$ State of Cr^{3+} in ruby and emerald.
398 Physical Review, 160, 307–312.

399 Klotz, S., Chervin, J.C., Munsch, P., and Le Marchand, G. (2009) Hydrostatic limits of 11
400 pressure transmitting media. Journal of Physics D: Applied Physics, 42, 075413.

401 Kottke, T., and Williams, F. (1983) Pressure dependence of the alexandrite emission
402 spectrum. Physical Review B, 28, 1923-1927.

403 Kraft, S., Knittle, E., and Williams, Q., (1991) Carbonate stability in the Earth's mantle: a
404 vibrational spectroscopic study of aragonite and dolomite at high pressures and
405 temperatures. Journal of Geophysical Research, 96, 17997-18009.

Always consult and cite the final, published document. See http:/www.minsocam.org or GeoscienceWorld

Mao, H.K., and Bell, P.M. (1986) Calibration of the ruby pressure gauge to 800 kbar under quasi-hydrostatic conditions. Journal of Geophysical Research, 91, 4673–4676.

Nestola, F., Ballaran, T.B., and Ohashi, H. (2008) The high-pressure C2/c–P2_1/c phase transition along the $LiAlSi_2O_6$–$LiGaSi_2O_6$ solid solution. Physics and Chemistry of Minerals, 35, 477–484.

Piermarini, G.J., Block, S., and Barnett, J.D. (1973) Hydrostatic limits in liquids and solids to 100 kbar. Journal of Applied Physics, 44, 5377-5382.

Pommier, C.J.S., Denton, M.B., and Downs, R.T. (2003) Raman spectroscopic study of spodumene ($LiAlSi_2O_6$) through the pressure-induced phase change from C2/c to P2_1/c. Journal of Raman Spectroscopy, 34, 769–775.

Redhammer, G.J., and Roth, G. (2004) Structural variation and crystal chemistry of $LiMe^{3+}Si_2O_6$ clinopyroxenes Me^{3+}= Al, Ga, Cr, V, Fe, Sc and In. Zeitschrift für Kristallographie, 219, 278-294.

Robinson, K., Gibbs, G.V., and Ribbe, P.H. (1971) Quadratic elongation: A quantitative measure of distortion in coordination polyhedra. Science, 172, 567–570.

Sangster, M.J.L., and McCombie, C.W. (1970) Calculation of phonon sidebands in emission spectra of V^{2+} and Ni^{2+} in MgO, Journal of Physics C, 3, 1498-1512.

Sanz-Ortiz, M.N., Rodriguez, F., Hernandez, I., Valiente, R., and Kuck, S. (2010) Origin of the ^2E-$^4T_2$ Fano-type resonance in Cr^{3+}-doped $LiCaAlF_6$: Pressure-induced excited-state crossover. Physical Review B, 81, 045114.

Syassen, K. (2008) Ruby under pressure. High Pressure Research, 28, 75–126.

Tanabe, Y., and Sugano, S. (1954) On the absorption spectra of complex ions, I. Journal of the Physical Society of Japan, 9, 753-766.

Taran, M.N., Ohashi, H., Langer, K., and Vishnevskyy, A.A. (2011) High-pressure electronic absorption spectroscopy of natural and synthetic Cr^{3+}-bearing clinopyroxenes. Physics and Chemistry of Minerals, 38, 345-356.

Taraschan, A.N., Taran, M.N., Rager, H., and Iwanuch, W. (2005) Luminescence spectroscopic study of Cr^{3+} in Brazilian topazes from Ouro Preto. Physics and Chemistry of Minerals, 32, 679-690.

Tribaudino, M., Nestola, F., Prencipe, M., and Rundlof, H. (2003) A single-crystal neutron-diffraction investigation of spodumene at 54 K. Canadian Mineralogist, 41, 521-527.

Ullrich, A., Schranz, W., and Miletich, R. (2009) The nonlinear anomalous lattice elasticity associated with the high-pressure phase transition in spodumene: A high-precision static compression study. Physics and Chemistry of Minerals, 36, 545–555.

Always consult and cite the final, published document. See http:/www.minsocam.org or GeoscienceWorld

Walker, G., El Jaer, A., Sherlock, R., Glynn, T. J., Czaja, M., and Mazurak, Z. (1997) Luminescence spectroscopy of Cr^{3+} and Mn^{2+} in spodumene ($LiAlSi_2O_6$). Journal of Luminescence, 74, 278–280.

Wamsley, P., and Bray, K. (1994) The effect of pressure on the luminescence of Cr^{3+}: YAG. Journal of Luminescence, 59, 11–17.

Williams, Q., and Jeanloz, R. (1985) Pressure shift of Cr^{3+}-ion-pair emission in ruby, Physical Review B, 31, 7449-7451.

Zheng, W.-C. (1995) Determination of the local compressibilities for Cr^{3}+ ions in some garnet crystals from high-pressure spectroscopy. Journal of Physics Condensed Matter, 7, 8351-8356.

Always consult and cite the final, published document. See http:/www.minsocam.org or GeoscienceWorld

Figure 1. Structures of the spodumene C2/c and $P2_1/c$ phases (color online). Notably, the Al-atoms are off-center in their octahedral sites in both phases. The primary difference between these two phases is a distortion of the Li-site, which also leads to a difference in the kink of the B-chain of tetrahedra, Modified from Pommier et al. (2003); crystal structures from Arlt and Angel (2000).

Figure 2. Representative luminescence spectra of spodumene on compression (a) to ~15 GPa and on decompression (b) to room pressure. The high-pressure phase transition produces a noticeable change in the luminescence spectra, and hysteresis of the phase transition is observed on decompression (most notably in the 2.5 GPa spectrum).

Figure 3. Pressure shift of the (a) R-lines (b) side-bands (color online). Note discontinuous shifts at ~3.2 indicating the C2/c to $P2_1/c$ high pressure phase transition. Closed symbols are data on compression, and open symbols on decompression, and error bars are smaller than the symbols. The main R_1 band is shown by downward facing triangles and the main R_2 band by upward facing triangles. Diamond symbols (red in on-line version) represent the $^4T_2$ emission.

Figure 4. Representative luminescence emission spectra of spodumene at various temperatures. The R-lines broaden and shift to longer wavelength (lower energy) and the intensity of the broad $^4T_2$-$^4A_2$ transition (relative to R_1) increases as temperature increases. The low-amplitude sharp features in the 77 K spectra are attributed to neighbor lines, juxtaposed with broader vibronic lines.

Figure 5. Fit of broad-band emission from the $^4T_2$ band as a function of pressure (color online). Note that it shifts to shorter wavelength (higher energy) and the intensity rapidly decreases as pressure increases dashed arrow (red in on-line version).

Figure 6. Tanabe-Sugano diagram for d^3 electron configuration of Cr^{3+} in octahedral symmetry showing the energy levels in weak and strong crystal fields. Cr^{3+} in spodumene is in a weak to intermediate strength field in the C2/c phase and in a strong crystal field in the $P2_1/c$ phase. Axes labels are incorporate the ligand field splitting parameter Δ (or 10 Dq), the Racah parameter B, and E is energy. Modified from Gaft et al. (2005) and Tanabe and Sugano (1954).

Figure 7. (a) R-line separation as a function of pressure. Inset shows the shift in quadratic elongation (Robinson et al., 1971) of the M1 site as a function of pressure, from Arlt and Angel (2000). (b) FWHM of R-lines as a function of pressure (R_2 circles, R_1 squares). Closed symbols are compression and open symbols are decompression, and error bars are smaller than the symbols. The scatter within the FWHM data on decompression in the low-pressure phase may be related to residual strain after the sample has been cycled through the phase transition.

Table 1. Assignment, wavelength and wavenumber of spectral features, offset of sidebands from R_1, and pressure shifts of R-lines, and sidebands which include both vibronic and N-

Always consult and cite the final, published document. See http:/www.minsocam.org or GeoscienceWorld

498 lines (neighbor lines due to Cr-Cr pair emission) in both the C2/c and $P2_1/c$ phases. *not
499 observed in the C2/c phase, reported wavelength and wavenumber are at ~3.2 GPa.

Always consult and cite the final, published document. See http:/www.minsocam.org or GeoscienceWorld

Figure 1

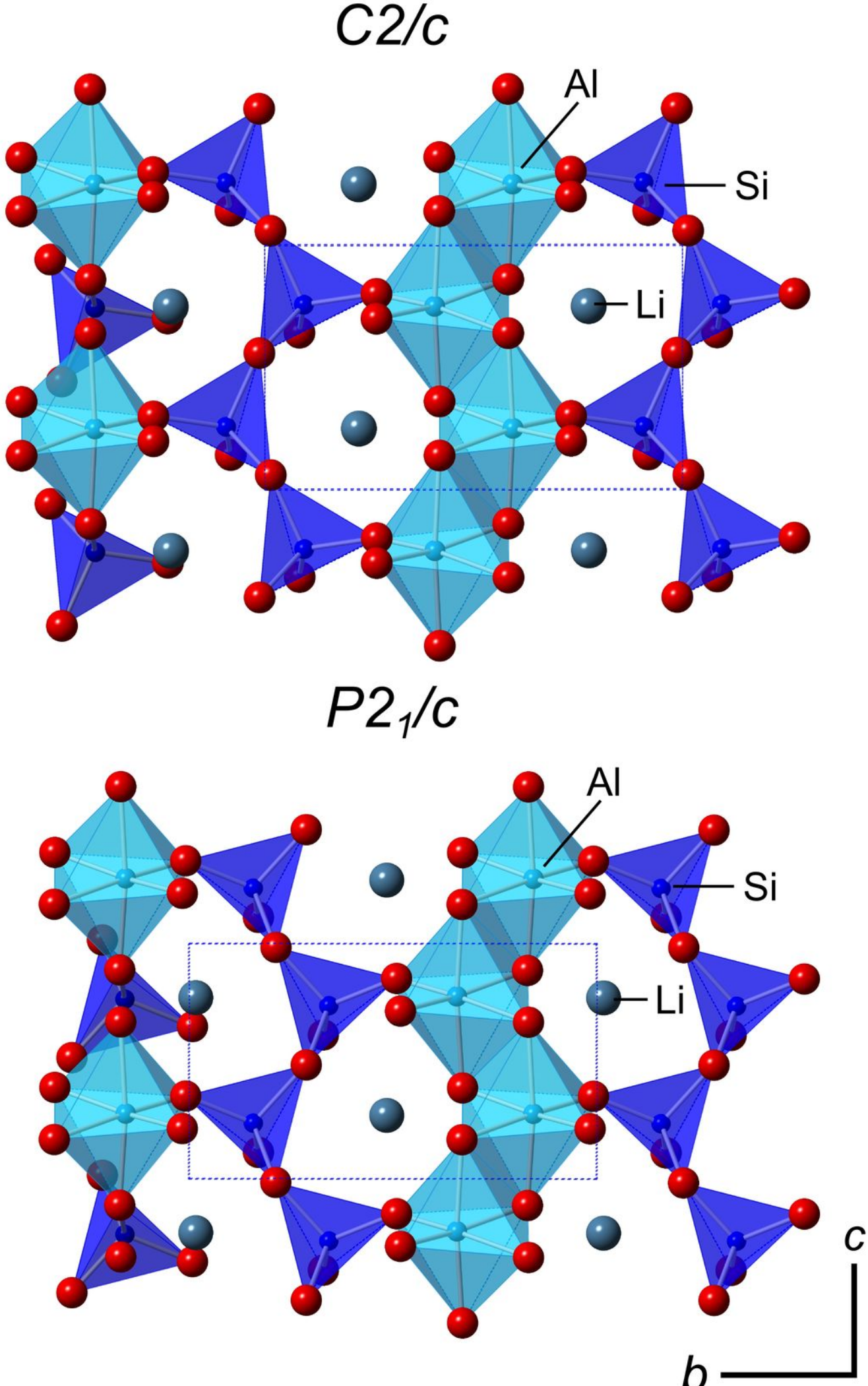

Figure 2a

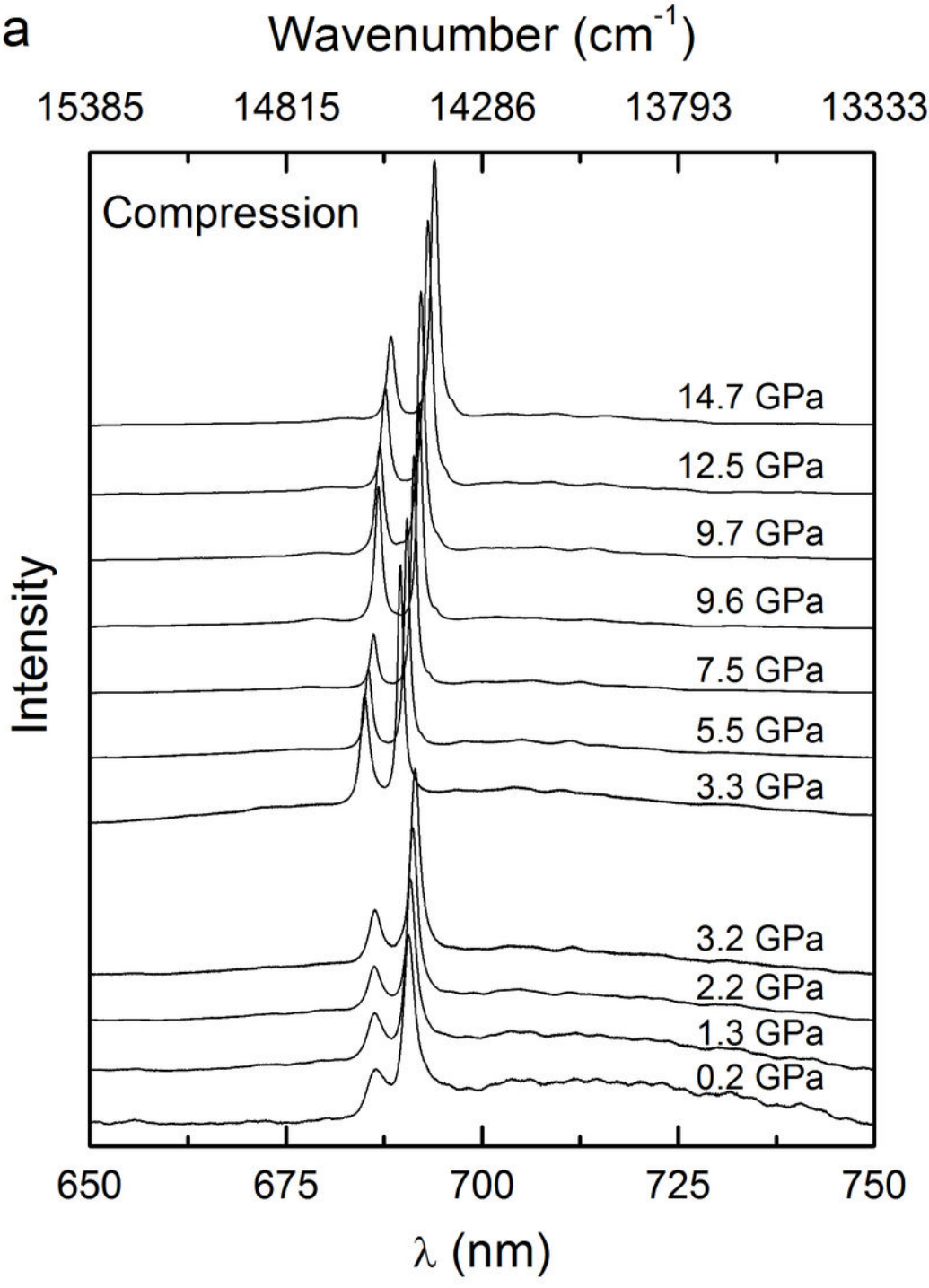
a
Wavenumber (cm-1)
15385
14815
14286
13793
13333
Compression
14.7 GPa
12.5 GPa
9.7 GPa
9.6 GPa
7.5 GPa
5.5 GPa
3.3 GPa
3.2 GPa
2.2 GPa
1.3 GPa
0.2 GPa
Intensity
650
675
700
725
750
λ (nm)

Figure 2b

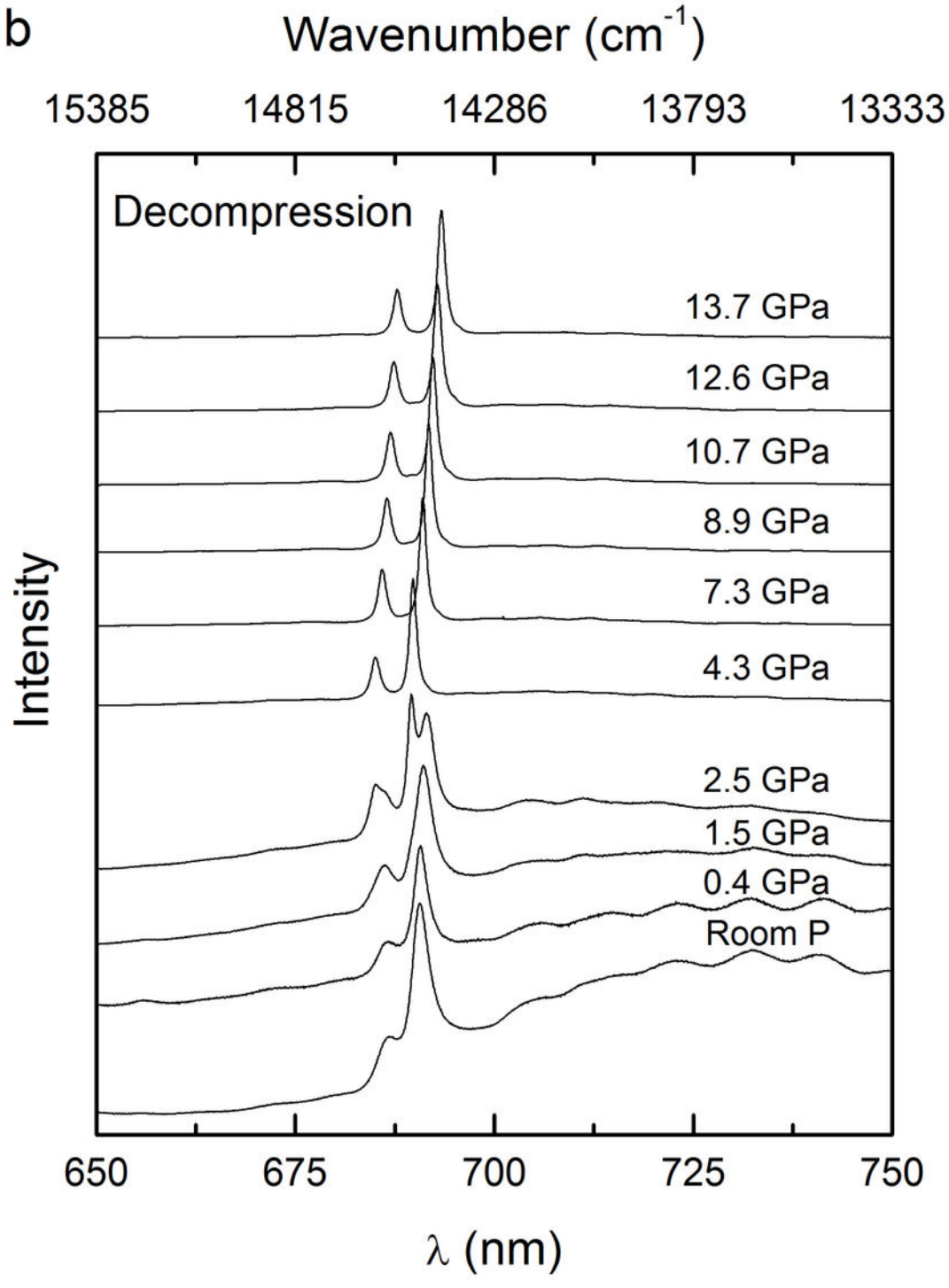
b
Wavenumber (cm-1)
15385
14815
14286
13793
13333
Decompression
13.7 GPa
12.6 GPa
10.7 GPa
8.9 GPa
7.3 GPa
4.3 GPa
2.5 GPa
1.5 GPa
0.4 GPa
Room P
Intensity
650
675
700
725
750
λ (nm)

Figure 3a

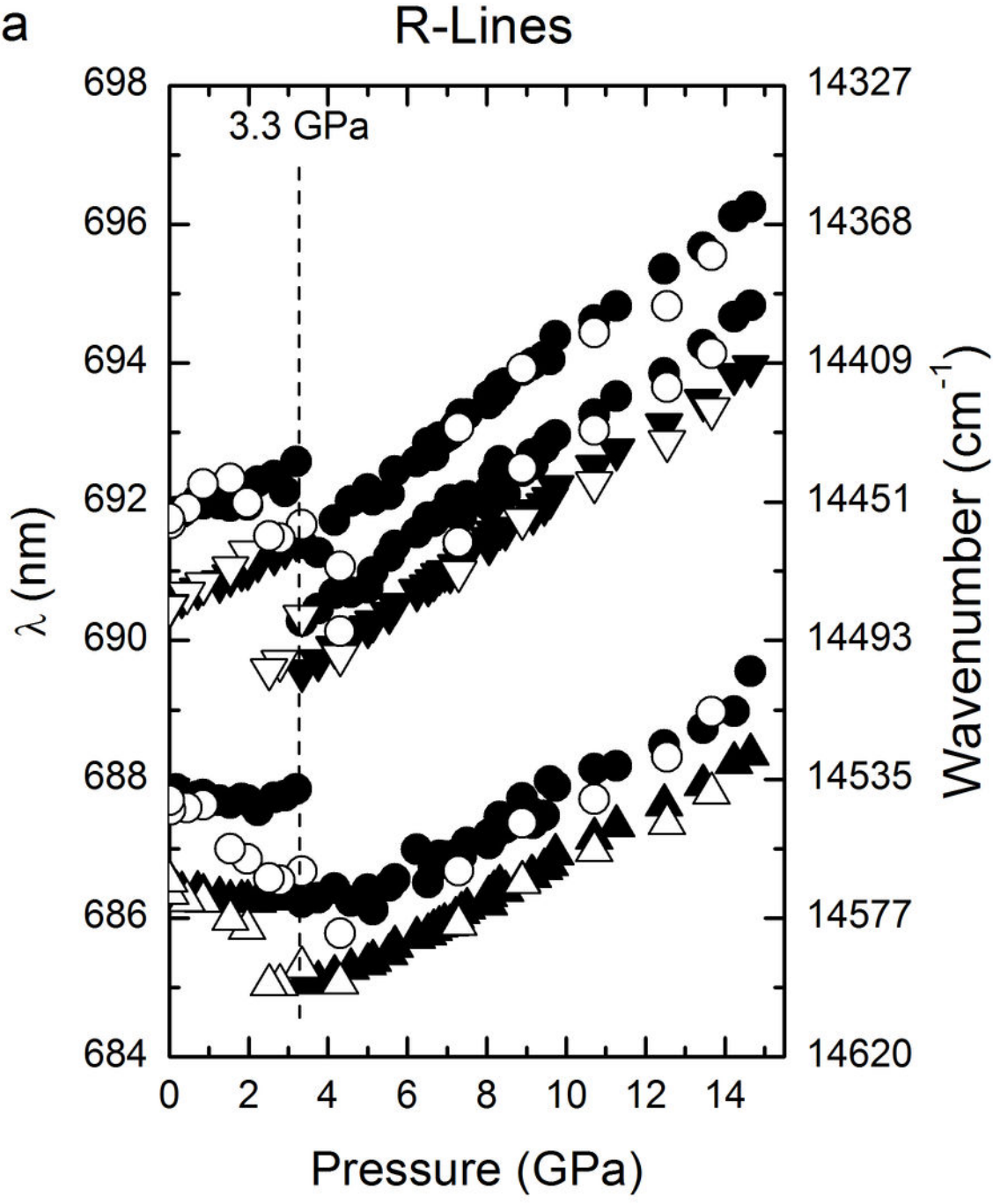
a
R-Lines
3.3 GPa
698
696
694
692
690
688
686
684
λ (nm)
14327
14368
14409
14451
14493
14535
14577
14620
Wavenumber (cm-1)
0
2
4
6
8
10
12
14
Pressure (GPa)

Figure 3b

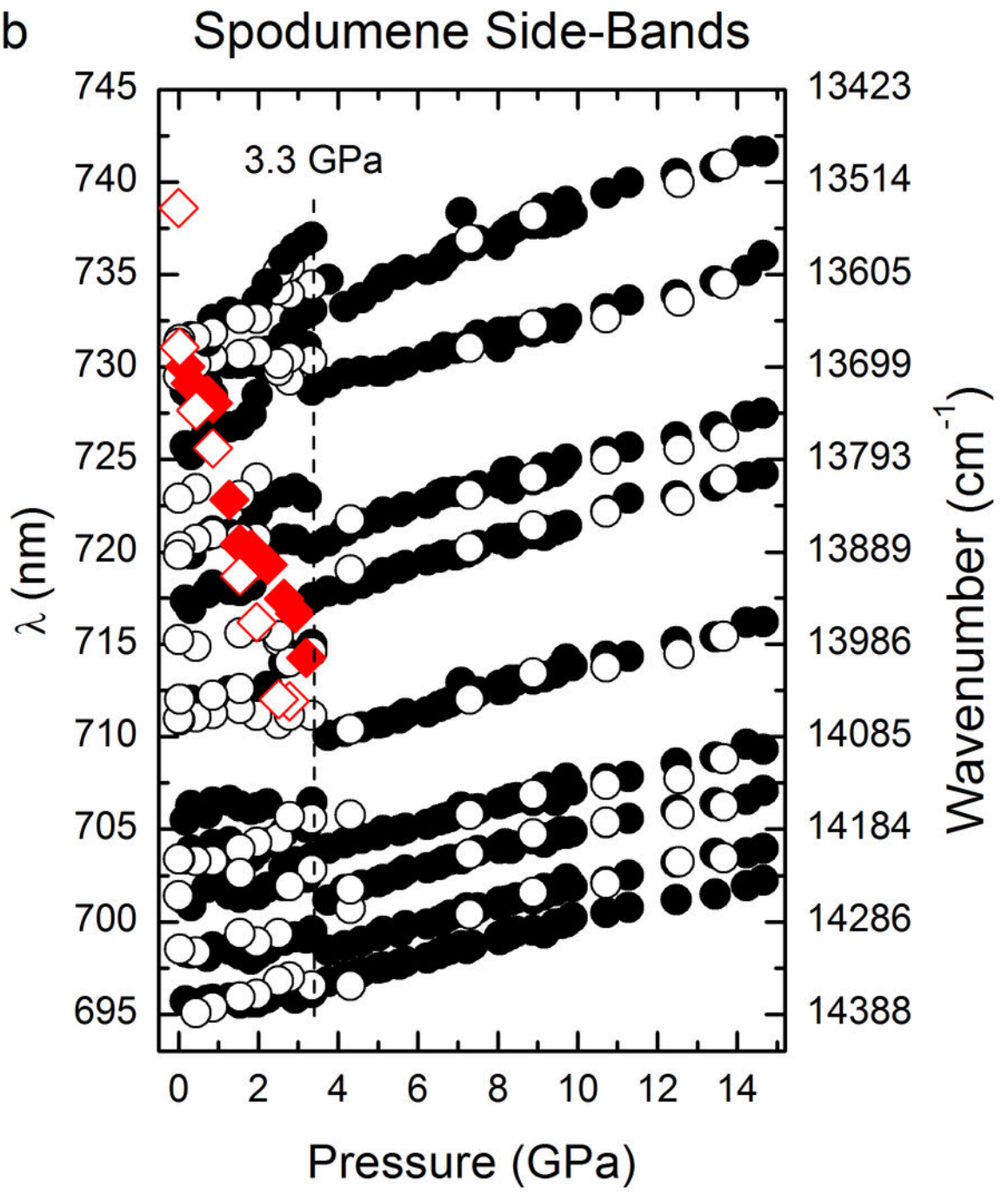
b
Spodumene Side-Bands
3.3 GPa
λ (nm)
Wavenumber (cm-1)
Pressure (GPa)
745
740
735
730
725
720
715
710
705
700
695
13423
13514
13605
13699
13793
13889
13986
14085
14184
14286
14388
0
2
4
6
8
10
12
14

Figure 4

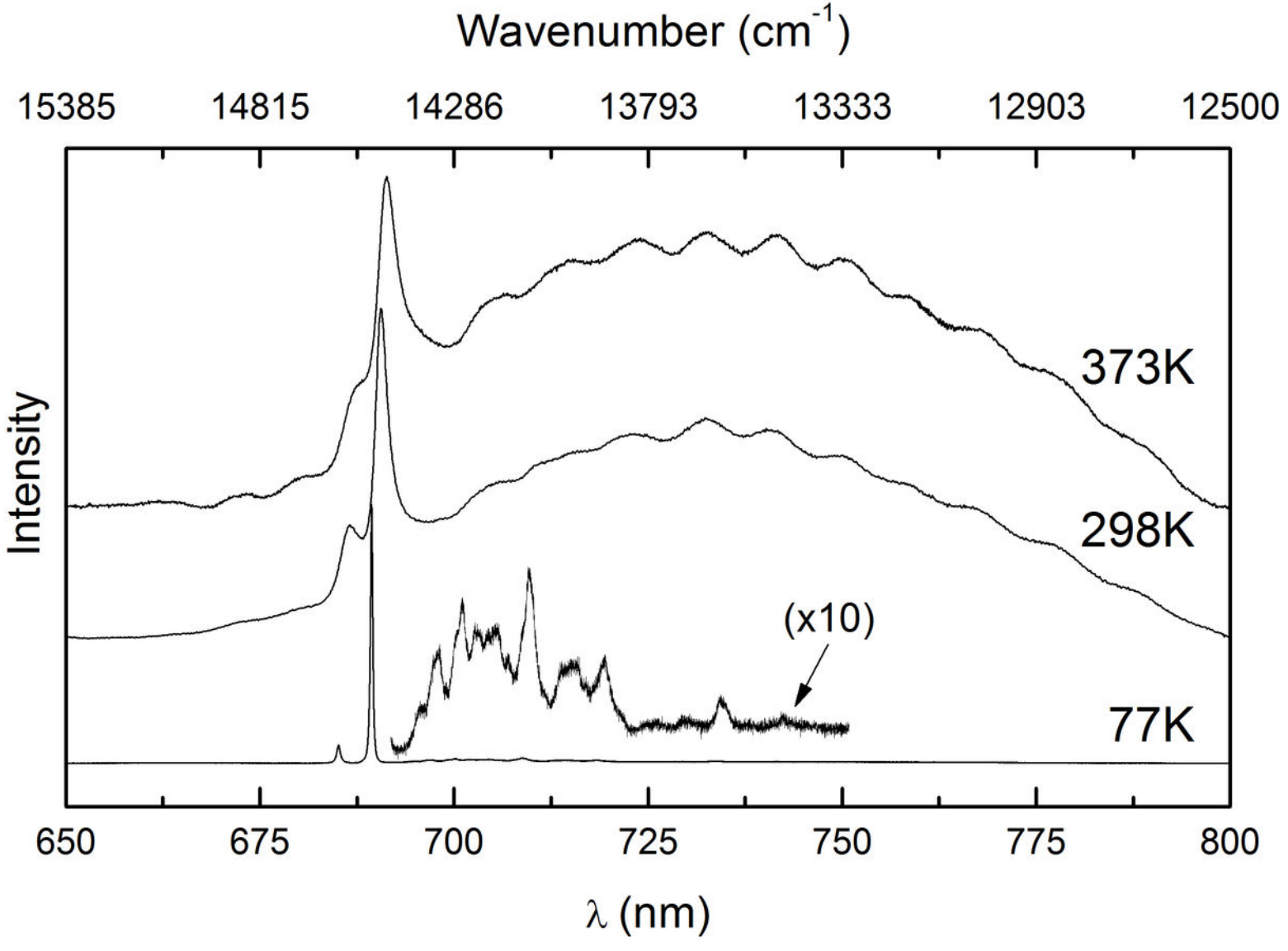
Wavenumber (cm-1)
15385
14815
14286
13793
13333
12903
12500
Intensity
373K
298K
(x10)
77K
650
675
700
725
750
775
800
λ (nm)

Figure 5

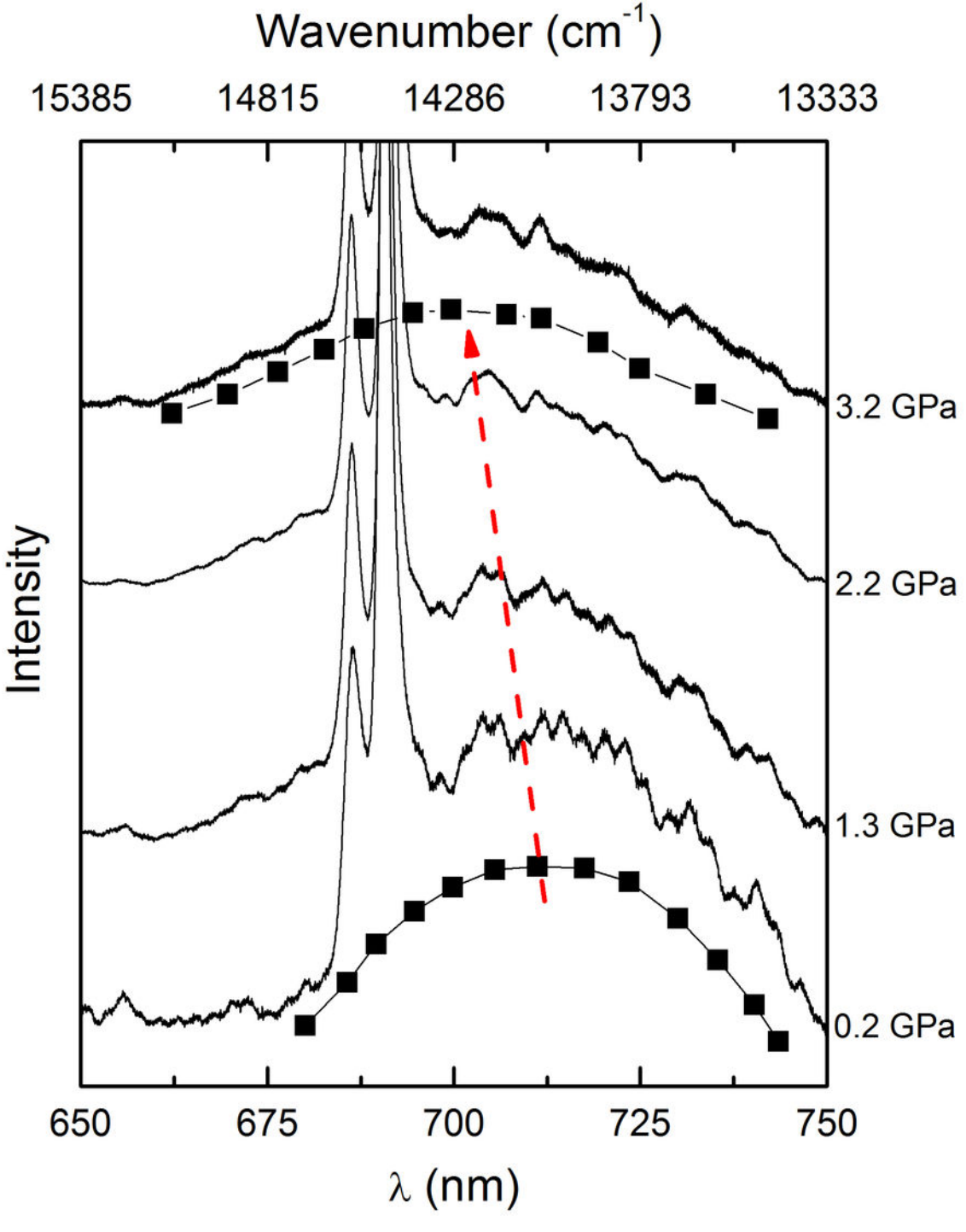
Wavenumber (cm-1)
15385
14815
14286
13793
13333
3.2 GPa
2.2 GPa
1.3 GPa
0.2 GPa
Intensity
650
675
700
725
750
λ (nm)

Figure 6

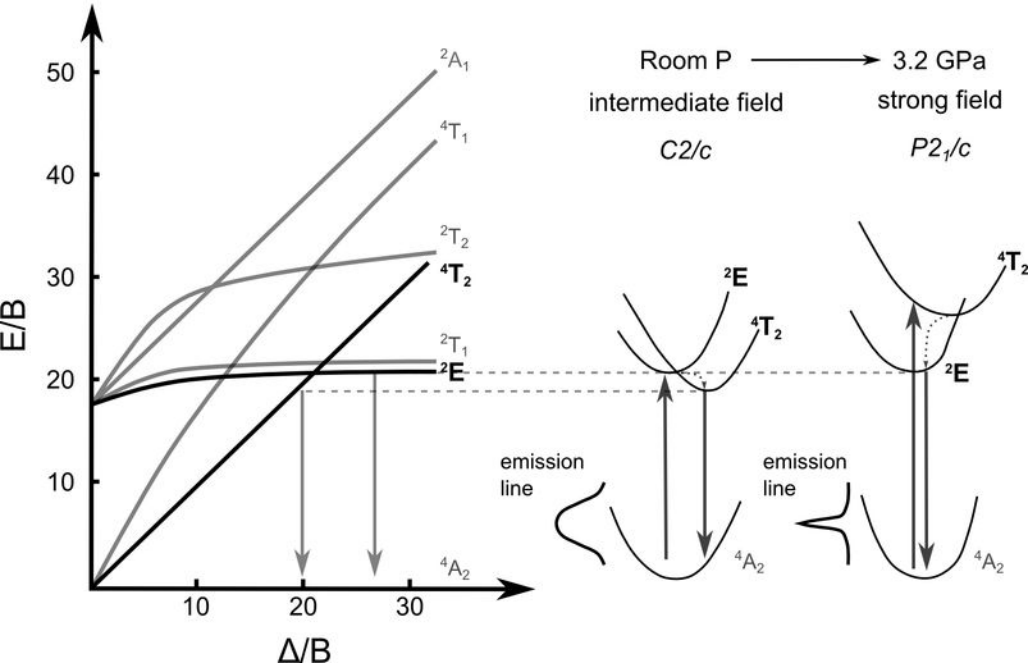
E/B
Δ/B
50
40
30
20
10
10
20
30
$^2A_1$
$^4T_1$
$^2T_2$
$^4T_2$
$^2T_1$
^2E
$^4A_2$
Room P
3.2 GPa
intermediate field
strong field
C2/c
P2₁/c
^2E
$^4T_2$
emission line
emission line
$^4A_2$
$^4A_2$

Figure 7a

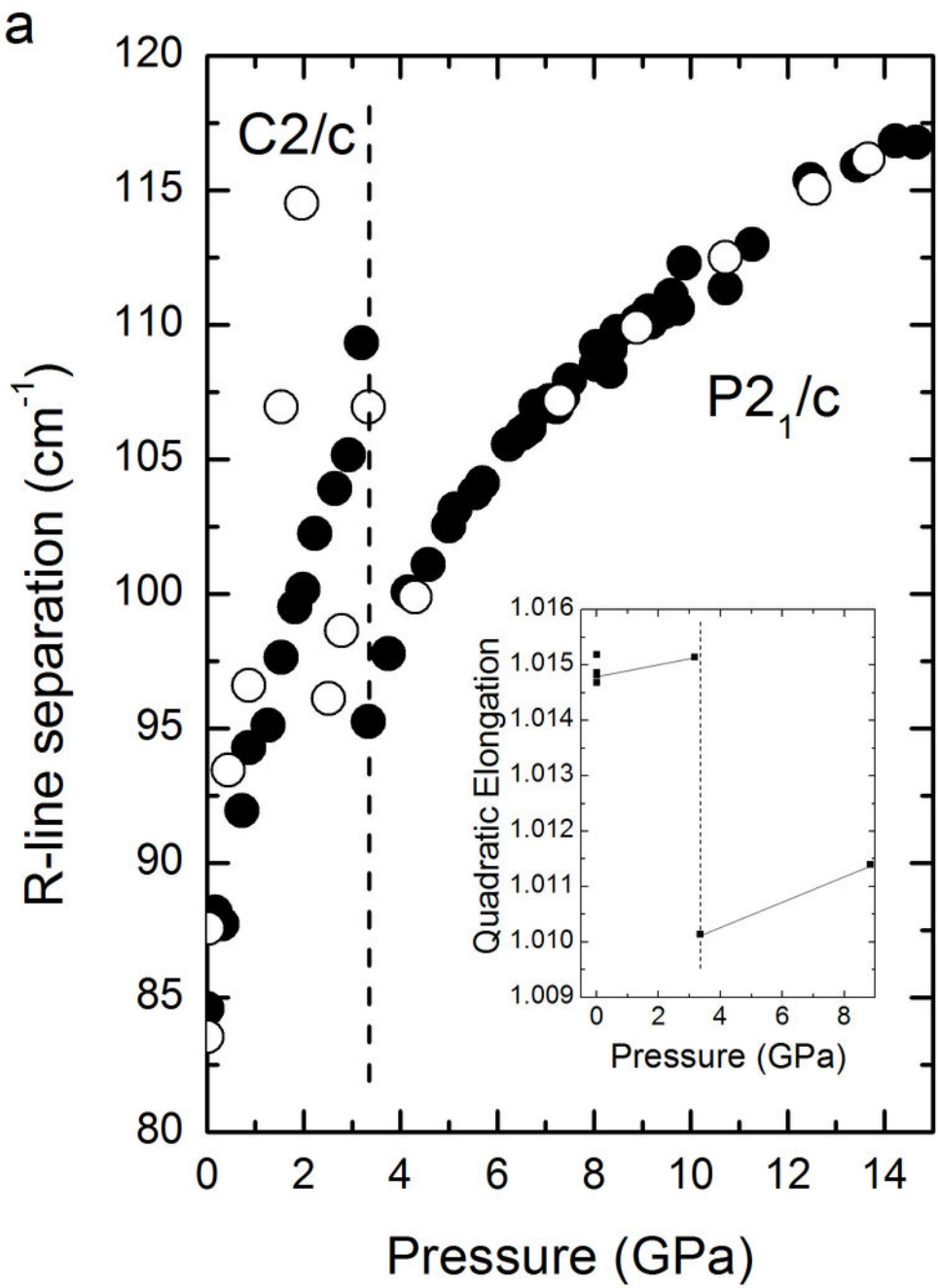
a
C2/c
P2$_1$/c
R-line separation (cm^{-1})
Pressure (GPa)
Quadratic Elongation
Pressure (GPa)

Figure 7b

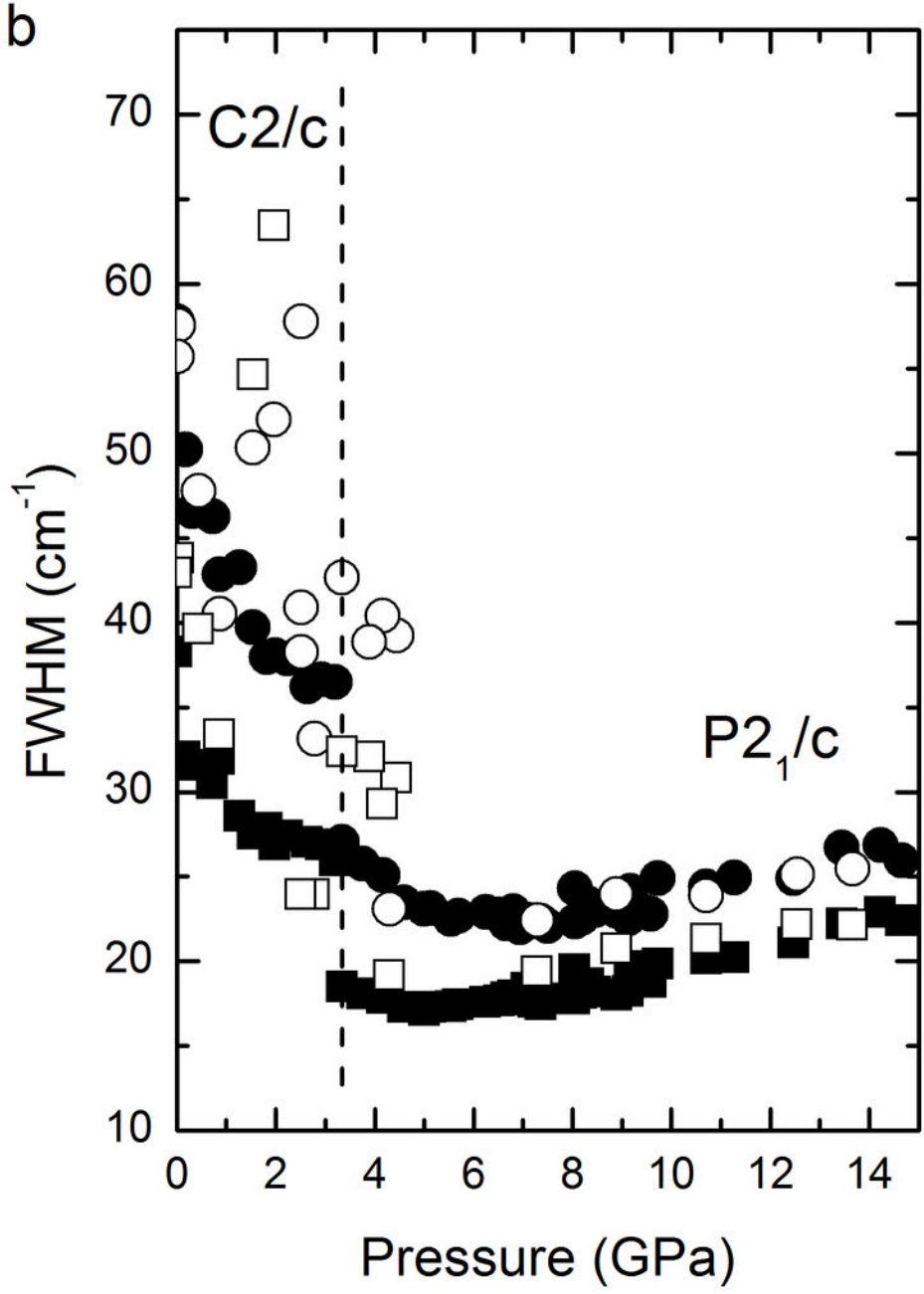
b
C2/c
P2$_1$/c
FWHM (cm^{-1})
Pressure (GPa)
10
20
30
40
50
60
70
0
2
4
6
8
10
12
14

Assignment	λ (nm)	ν (cm^{-1})	Δν from R_1 (cm^{-1})	*C2/c* *dν/dP* (cm^{-1}/GPa)	*$P2_1/c$* *dν/dP* (cm^{-1}/GPa)
R_2	686.54 (primary)	14565.8		1.4 (±0.3)	-6.5 (±0.1)
	687.68 (shoulder)	14541.6		0.6 (±0.4)	-6.1 (±0.2)
R_1	690.55 (primary)	14481.2		-5.2 (±0.2)	-8.2 (±0.1)
	691.79 (shoulder)	14455.3		-3.1 (±0.7)	-8.3 (±0.2)
	691.40*	14463.4*	-	-	-9.1 (±0.1)
N-Line	695.72	14373.6	107.6	-3.3 (±0.7)	-9.7 (±0.2)
N-Line	698.35	14319.5	161.7	-5.4 (±1.9)	-10.1 (±0.2)
	701.17	14261.9	219.3	-6.5 (±0.7)	-9.9 (±0.2)
	703.39	14216.9	264.3	3.9 (±2.7)	-9.8 (±0.2)
	705.51	14174.1	307.1	-3.8 (±2.9)	-
N/Vibronic?	711.40	14056.8	424.4	-18.3 (±3.5)	-10.9 (±0.3)
Vibronic	717.39	13939.4	541.8	-26.3 (±3.8)	-10.3 (±0.3)
Vibronic	720.29	13883.3	597.9	-21.9 (±2.7)	-13.5 (±0.5)
	725.73	13779.2	702.0	-37.5 (±3.4)	-10.8 (±0.2)
	728.72	13722.7	758.5	-25.2 (±2.6)	-10.9 (±0.2)
$^4T_2$-$^4A_2$	730.02	13698.3	783.0	+100.5 (±7.2)	-
	731.48	13670.9	810.3	-33.6 (±3.3)	-